Moriam, Kaniz; Azevedo, Catarina; Fateixa, Sara; Bernardo, Fábio; Sixta, Herbert; Evtuguin, Dmitry V.

Modification of regenerated cellulose fibres by cork-derived suberin and the cutin fraction from grape skins

Published in:
Carbohydrate Polymer Technologies and Applications

DOI:
10.1016/j.carpta.2024.100613

Published: 01/12/2024

Document Version
Publisher's PDF, also known as Version of record

Carbohydrate Polymer Technologies and Applications 8 (2024) 100613

Contents lists available at ScienceDirect

Carbohydrate Polymer Technologies and Applications

journal homepage: www.sciencedirect.com/journal/carbohydrate-polymer-technologies-and-applications

Modification of regenerated cellulose fibres by cork-derived suberin and the cutin fraction from grape skins

Kaniz Moriam [a,b], Catarina Azevedo [c], Sara Fateixa [c], Fábio Bernardo [c], Herbert Sixta [a], Dmitry V. Evtuguin [c,*]

[a] Department of Bioproducts and Biosystems, School of Chemical Engineering Aalto University, P.O Box 16300, Espoo, FI-00076 Aalto, Finland
[b] Hatsopoulos Microfluids Laboratory, Department of Mechanical Engineering, Massachusetts Institute of Technology, Cambridge MA, USA
[c] CICECO, Department of Chemistry, University of Aveiro, Campus Universitário de Santiago, 3810-193 Aveiro, Portugal

ARTICLE INFO

Keywords:
Ioncell fibres
Suberin
Cutin
Ionic liquid, Hydrophobisation

ABSTRACT

Regenerated cellulose fibres from dissolving pulp are a versatile alternative to cotton fibres on the path to the sustainable textile industry. In this study, cellulose fibres obtained by the Ioncell-F® process (Ioncell fibres) were modified by adding 10 % (w/w) of suberin compounds isolated from cork (SUB) or a cutin fraction from grape skins (CUT) in the spinning dope. Although both SUB and CUT modified fibres revealed higher hydrophobicity than unmodified fibres, fibres doped with CUT showed better waterproof performance than those doped with SUB. This was explained by the better retention of CUT than SUB on the regenerated fibres and by the higher hydrophobicity of CUT. Differences in the strength properties of Ioncell fibres obtained by pilot-scale dry-jet wet spinning were related to their physical structure, whereas dirt repellence and susceptibility to enzymatic hydrolysis depended on the occurrence and amounts of retained CUT or SUB.

1. Introduction

The growing needs of the textile industry for natural fibres, mainly cotton, can no longer be met by simple increasing its cultivation due to economic and environmental concerns (Björquist et al., 2018; Mollaee et al. 2019; Shen et al., 2010). In fact, global cotton production is limited to around 25-26 million tons per year for the last three decades (Statista 2024). The resulting gap between natural fibre production and consumption is being addressed by increasing the production of regenerated cellulose (rayon) from various plant materials as technically and economically viable alternative (Hummel et al. 2016; Mendes et al. 2021; Zhang et al. 2017). Currently, around 9.5 million tons of dissolving cellulose are used to produce rayon, mainly viscose (Food and Agriculture Organization of the United Nations, 2022). Although viscose is the main type of regenerated fibres, its consumer properties are still significantly inferior to those of cotton (Asaadi et al. 2016; Mendes et al. 2021; Michud et al. 2016a). In addition, viscose production implies the use of hazardous reagents (CS_2 and strong alkali) that imply environmental problems. Alternative methods of obtaining rayon fibres dealing with the direct dissolution of cellulosic fibres in appropriate solvents are free from most of these drawbacks (Firgo et al., 1996; Hummel et al. 2016; Zhang et al. 2017). Among numerous direct cellulose solvent systems proposed, N-methyl morpholine-N-oxide (NMMO) and 1,5-diazabicyclo [4.3.0] non-5-ene acetate ([DBNH][OAc]) showed the most promising practical results being realized on industrial (Lyocell® process using NMMO) (Fink et al. 2001; Firgo et al., 1996) or pre-industrial (Ioncell® process using [DBNH][OAc]) scales (Mendes et al. 2021; Sixta et al. 2015). Both methods apply the dry-jet wet spinning concept and water coagulation bath with posterior recuperation of cellulose solvent (NMMO in Lyocell® and [DBNH][OAc] in Ioncell®) (Firgo et al., 1996; Parviainen et al. 2015; Stepan et al., 2016). However, Ioncell fibres revealed properties comparable to those of cotton and superior to those of lyocell and viscose fibres (Asaadi et. al., 2016; Michud et al., 2016b; Elsayed et al., 2021).

Another advantage of the Ioncell® and Lyocell® processes over viscose production is the possibility of modifying the fibres in the process of their regeneration as an alternative to the post-modification approach. Thus, modifying agents can be dissolved in the dope together with the cellulose pulp and deposited on the fibres during their formation and spinning. Among modifying agents, those that provide rayon with lacking properties such as hydrophobicity, fluorescence, conductivity, resistance to microbiological attack or affinity to specific

* Corresponding author.
E-mail address: Dmitrye@ua.pt (D.V. Evtuguin).

https://doi.org/10.1016/j.carpta.2024.100613
Received 30 September 2024; Received in revised form 19 November 2024; Accepted 20 November 2024
Available online 22 November 2024

surfaces are commonly applied (Edgar and Zhang, 2020; Ferrero and Periolatto, 2013; Huang et al., 2018, 2019; Makarov et al. 2018; Mendal et al. 2016; Moriam et al. 2021). Modified rayon can also be used as a source for the production of carbon fibres (Mikkelä et al. 2020). Regarding the hydrophobic and antimicrobial properties, the bio-inspired approach regarding the modifying agents has prevailed due to human safety and biorefinery considerations. Thus, triterpenes and triterpenoids (Huang et al., 2018, 2019; Makarov et al. 2018; Moriam et al. 2021), lignin (Ma et al., 2015; Protz et al., 2021) and waxes (Forsman et al 2020) have been reported as suitable agents for these purposes. Suberin and cutin are two natural polyesters that exhibit hydrophobicity and antimicrobial properties required by plants (Correia et al. 2020; Heredia 2003; Li-Beisson et al. 2016) and have not yet been reported for the purpose of modifying regenerated cellulosic fibres. Meanwhile these substances inspire confidence in the safety of their use in contact with the human body and food, being also an integral part of fruits and vegetables.

In this work, for the first time, depolymerised suberin (SUB) from cork and cutin fraction from grape skins soluble in dichloromethane (CUT) were introduced into the composition of a dope containing soluble eucalyptus pulp in [DBNH][OAc] with the aim of its subsequent precipitation on the single regenerated Ioncell fibres to acquire them hydrophobic properties. The retention of each hydrophobising agent on fibres was estimated and the occurrence and allocation of deposited SUB and CUT were evaluated by Fourier transform infrared spectroscopy (FTIR), confocal Raman spectroscopy and atomic force microscopy (AFM). To evaluate the effect of fibre modification on their structure and mechanical properties, the physical structure of the fibres was studied and related to the tensile strength of the regenerated fibres. The surface properties of the modified fibres were assessed by X-ray photoelectron spectroscopy, adsorption isotherms and contact angle measurements being further correlated with waterproofing and resistance to cellulolytic enzymes attack. The yarn spinnability of undoped and doped rayon fibres was compared. Knitted fabrics were produced for demonstration purposes and their stain resistance status was examined in relation to acquired fibre hydrophobicity.

2. Materials and methods

2.1. Materials

Eucalyptus (*Eucalyptus globulus*) sulphite dissolving pulp (intrinsic viscosity of 510.0 cm^3/g, residual pentosane content of 2.6 % (w/w) and α-cellulose content of 92.9 % (w/w)) was supplied by the pulp company Caima, S.A. (Constância, Portugal). The ionic liquid (IL) [DBNH][OAc] was synthesized using equimolar amount of acetic acid (100 %, from Merk Chem. Comp., Germany) and 1,5-diazabicyclo [4.3.0] non-5-ene (DBN, 99 %, supplied by Fluorochem Ltd., Basel, Switzerland). The LR White Resin was supplied by Agar Scientific Ltd. (Stansted, UK). Suberin was isolated from cork particles of 40-60 mesh supplied by Amorim & Irmãos, S.A. (Santa Maria de Lamas, Portugal). The grape skins from mixed pomaces of different grape varieties were supplied by wine cooperative from the Douro region (Portugal).

2.2. Isolation of suberin and cutin

Suberin extracts were obtained by alkaline methanolysis with 2 % sodium methoxide according to previously published procedure (Branco et al., 2020). The composition of isolated suberin is presented in Table S1 (Supplementary data). The analysis of depolymerised suberin was carried out by gas chromatography coupled with mass-spectrometry detector (GC-MS) as trimethylsilyl (TMS) derivatives (Branco et al. 2020). Grape skins were separated from stalks and seeds and firstly extracted by water (solid-to-liquid ratio of 10) at 100 °C for 1 h (Mendes et al. 2013b). The skins extracted with water were dried at 40 °C for 12 h. The cutin fraction was isolated from the dried grape skins by extraction with dichloromethane for 6 h in Soxhlet (Mendes et al. 2013a). The composition of the extracted cutin fraction is presented in Table S2 (Supplementary data). The analysis of the extract was carried out by GC-MS as TMS derivatives (Mendes et al. 2013a).

2.3. Preparation of dopes

The ionic liquid ([DBNH][OAc]) was melted at 80 °C and added to a preheated kneader at 80 °C. In the case of additive (suberin or cutin) incorporated dope, first the additive was added to ionic liquid and stirred for 30 min at 80 °C (30 rpm). Visually, suberin was easier dissolved than cutin. Once the additive was dissolved in the ionic liquid, the dissolving pulp was added and blended for ca 90 min at 80 °C (30 rpm) at reduced pressure (10-30 mbar). The concentrations of suberin and cutin were adjusted to ca 10 % (w/w). The obtained solutions were filtered through a hydraulic press filter device (metal filter mesh with 5-6 μm absolute fineness, Gebr. Kufferath AG, Germany) at 80 °C to remove undissolved substrates. The prepared filtered dope was solidified upon cooling overnight. The moisture content in the pulp (about 8 %) was kept constant to ensure approximately equal water content in a dope.

2.4. Spinning

The solidified dope was heated to 80 °C in the spinning cylinder to form a highly viscous fluid. Multi-filaments were spun with a customised laboratory piston spinning system (Fourné Polymer Technik, Germany). The molten solution was extruded through a 200-hole spinneret with a capillary diameter of 100 μm and a capillary length to diameter ratio (L/D) of 0.2. After the fluid filaments had passed an air gap of 10 mm, they were coagulated in a water bath (8-12 °C) being further guided by Teflon rollers to the godet couple. The extrusion velocity ([L]/[t]) was set to 3.5 m min^{-1}. The spun fibres were washed with hot water (80 °C) to eliminate the residual ionic liquid and air-dried.

2.5. Preparation of non-woven sheets

Ioncell fibres were shortened into ~ 4 mm cuttings and suspended in distilled water until ca. 2 % consistency. The fibre suspension was filtered off on the glass filter of 5-cm diameter and dried at 50 °C in the ventilated oven. The sheet grammage varied from 70 to 75 g/m^2. Sheets were conditioned at 25 °C and 60 RH for 48 h before the analyses.

2.6. Ioncell fibres analysis

2.6.1. Analysis of the additive content

The amount of additive was calculated as a percentage of the dry sample after ca 2 g Ioncell fibres extraction in Soxhlet apparatus for 6 h using methanol (250 mL) as a solvent. The results were averaged from two parallel extractions. The percentage of additive was calculated as follows: amount of additive (%) = (amount of extracted additive (g) × 100)/(Initial amount of fibres(g)).

2.6.2. Birefringence

Fibre's birefringence was measured using a polarised light microscope (Zeiss Axio Scope, Zeiss AG, Germany). The linear density of the fibres was measured using the Favigraph tester and then the fibres were placed under tension between two pieces of double-sided tape on a microscope slide. The optical retardation was determined in three different places along the fibre. Birefringence (Δn) was calculated using the optical retardation of polarised light divided by the diameter. Total orientation (ft) was obtained via dividing Δn by the maximum value of birefringence (0.062) for cellulose (Lenz et al. 1994).

2.6.3. X-ray Photoelectron Spectroscopy (XPS)

The surface composition of ioncell fibres was assessed by XPS using

an AXIS Ultra electron spectrometer (Kratos Analytical, Manchester, U. K.) at low power setting of 100 W. Fibre bundles were attached onto the sample holder being partially outside the holder, in order to avoid a background signal. Samples were pre-evacuated overnight to secure stable ultra-high vacuum conditions during the experiment. Furthermore, a clean reference sample of 100 % cellulose filter paper was added to each sample batch to monitor possible contaminations. Each measurement location was optimised manually. Both low resolution wide scans and high-resolution C 1s and O 1s regions were recorded in different locations. Elemental compositions were determined from wide scans, and the carbon chemistry was evaluated from C 1s regional scans, using Casa XPS software and C 1s component fit tailored for cellulose.

2.6.4. Sorption isotherms

Water sorption isotherms of Ioncell fibres were obtained at 25 °C and at relative pressure in the range between 0.05 and 0.95 using the Dynamic Vapor Sorption Analyzer (DVS Adventure, Surface Measurement Systems Ltd., Wembley, UK). The results from three parallel experiments were averaged. The experimental sorption data, such as an equilibrium moisture content, X_{eq}, and water activity, a_w (or relative pressure), were fitted into the Guggenheim-Anderson-de Boer (GAB) model that is valid for high relative pressures ($P/P_0 \leq 0.90$) and adequately describes for surface affinity studies of cellulosic pulps (Portugal et al. 2010). GAB model is described by the following equation:

$$X_{eq} = \frac{X_m\ C\ K\ a_w}{((1 - K\ a_w)(1 + (C - 1)K\ a_w))} \quad (1)$$

where C and K are the GAB model parameters that are related to the heat of sorption in monolayer and multilayer, respectively, and X_m is the monolayer capacity. C, K and X_m were estimated from the experimental results by nonlinear regression analysis of GAB model.

2.6.5. Wide angle X-ray scattering (WAXS)

X-ray diffraction scattering analysis of fibres was carried out on a Philipps XPert MPD diffractometer using Cu-Kα source ($\lambda = 0.154$ nm) in the 2θ range 2-40° and scanning step width of 0.02°/scan. Ioncell fibres were analysed as textured samples. Fibres were cut into smaller ones (ca 2-4 mm) by scissors. The cut fibres were pressed into pellets of 1.2 cm diameter and about 1 mm thickness by pressing at 50 Mpa for 30 s.

The baseline of scattering profile was corrected using spline interpolation. The diffractograms were analysed using FullProf Suite V. 6.3 software. The average crystal widths in 110 plane direction (D_{110}) were calculated using known Scherrer equation (Klemm et al. 1998):

$$D_{110} = \frac{K\ \lambda}{\beta_{hkl}\cos\theta} \quad (2)$$

where K = 0.90 is the shape factor, λ is the X-ray wavelength (0.154 nm), β_{hkl} is the full width of half maximum (FWHM) of the diffraction peak in radians and θ is the diffraction angle of the peak.

The index of cellulose crystallinity (*CrI*) was calculated according to Segal's approximation as follows:

$$CrI = \frac{I_c - I_a}{I_c} \quad (3)$$

where I_c and I_a are the intensity of the peak at ca. $2\theta = 20°$ corresponding to crystalline reflection (110 lattice) and the intensity of amorphous halo at ca. 18.5°, respectively.

2.6.6. Contact angle measurement

Contact angle (CA) measurements were carried out on a Contact Angle System OCA20 goniometer (Data Physics Instruments, Filderstadt, Germany) equipped with a CCD camera and SCA20 software, using the sessile drop method applying 3 μL micro-drops of distilled water. The static contact angle on the non-woven sheets was measured for 30 s, which included the time to reach an equilibrium state (ca 15 s). At least 10 determinations were done per each sample and the obtained results were averaged. The contact angles of the SUB and CUT extracts were evaluated by applying a thin layer of them to the glass.

2.6.7. Enzymatic hydrolysis

For comparison reasons, Ioncell fibres without and with additives were hydrolysed using a commercial endo-cellulase (E.C.# 3.2.1.4) from *Trichoderma viride* (C9422, 9 U mg^{-1}, from Sigma–Aldrich Co., St. Louis, MO) following a previously described methodology (Ferreira et al. 2011). In a typical trial, ca 150 mg of cut fibres were dispersed in 35 mL of 0.05 M sodium acetate buffer (pH 5) being swollen for 1 h in the reactor at 40 °C. The hydrolysis started after the addition of cellulase (ca 9 U mg^{-1} fibres) at constant temperature (40 °C) and was monitored by determination of reducing sugars (RS) release along the hydrolysis (0.50 mL aliquot per each time point), which were quantified with 3,5-dinitrosalicylic acid (DNS), using glucose as the calibration standard.

2.6.8. AFM analysis

Atomic force microscopy (AFM) analysis of Ioncell fibres was carried out in tapping mode on a combined Raman-AFM-SNOM confocal microscope WITec alpha300 RAS$^+$ (WITec, Ulm, Germany), using a tip-cantilever silicon reflex-coated (NC tips) with a spring constant of k = 42 N m^{-1} and a resonance frequency of 285 kHz. The scanning areas were 2.5 μm × 2.5 μm (256 points per line × 256 lines per image) or 1.0 μm × 1.0 μm (128 points per line × 128 lines per image) scanned (and retraced) at a rate of 1 s/line. The surface roughness and arithmetic mean height (SA) were evaluated using the software Control 5.3$^+$.

2.6.9. Infrared spectroscopy

Infrared spectra of fibre bungles were acquired using a FTIR System Spectrum BX (PerkinElmer, Massachusetts, USA), coupled with a universal attenuated total reflection (ATR) sampling accessory, in absorbance mode from 4000 to 500 cm^{-1} with a 4 cm^{-1} resolution.

2.6.10. Confocal Raman analysis

The fibre samples were embedded with the LR White Resin, being oriented in the longitudinal direction in a closed gelatine capsule and cured in the oven at 105 °C for 6 h. Transverse sections approximately 2 μm thick were cut using a microtome (Reichert-Jung 2050 Super Cut Microtome, LabMakelaar Benelux B.V., Nederland). The obtained slices collected in the water container were deposited on the glass plate and fixed by drying. Raman spectra and images were acquired in a combined Raman-AFM-SNOM confocal microscope WITec alpha300 RAS$^+$ (WITec, Ulm, Germany). A Nd:YAG laser operating at 532 nm was used as excitation source with the power set between 1 and 1.8 mW. Raman imaging was performed by taking several Raman spectra in a uniform grid with different areas. The integration time for each spectrum was 0.2 s for a large area of 100 μm x 100 μm (40000 spectra), approximately 180 min with a 10x objective in the range between 0 and 3700 cm^{-1}. The Raman data were analysed using the command True Component Analysis (WITec Project 5.3$^+$) to create the combined Raman image. The True Component Analysis uses a basic analysis algorithm to fit the measured spectrum at each pixel as a linear combination of the reference library spectra using a least squares method. The Raman spectra of fibres, resin, and additive (CUT) were used to build a True Component reference library. Application of the True Component linear combination model to the hyperspectral dataset resulted in a component distribution image for each library component. The intensity of each pixel in the distribution image is determined by the degree of membership to a particular component by fitting the spectral response at the specific pixel with the reference library spectra. This was given an arbitrary value between 0 and 1, where a score value of 0 represents the absence of a component in a pixel and a score value of 1 demonstrates 100 % presence of a component. False-colour chemical images are the overlap of the Raman images for each component (red for the resin, blue for the fibres and green for the additive).

2.6.11. Image analysis

The Ioncell fibres were attached to the carbon tape and the images were acquired on a Hitachi TM 4000 Plus SEM microscope e (Hitachi, Tokyo, Japan) equipped by BSE detector and operated at 15 kV under vacuum of 30 Pa.

2.7. Yarn spinning and knitted fabrics cleanability

Fibres were opened (Trash Analyzer 281C, Mesdan Lab, Mesdan S.p.A., Italy) separately and conditioned (20 ± 2 °C, 65 ± 2 % RH) overnight to reduce electrostatic charges during the yarn spinning. The opened fibres were carded (Carding Machine 337A, Mesdan Lab, Mesdan S.p.A., Italy) to obtain a fibre web which was formed into a sliver. It was further elongated with a draw frame (Stiro Roving Lab 3371, Mesdan Lab, Mesdan S.p.A., Italy) and formed into a false-twist roving. The yarn was spun with a ring spinning machine (Ring Lab 82BA, SER. MA.TES srl, Italy), yarn twist direction: Z; twists per meter: 650 for the reference yarn, and ca 700 for modified with suberin and cutin yarns. The knitted fabrics were made in accordance with ISO 105-C06:2010 standard. Tensile testing of spun yarns (tenacity (cN/tex) and elongation at break (%) was measured by a MTS 400 tensile tester equipped with a 50 N load cell having a gauge length of 250 mm and a test speed of 250 mm/min. The yarn was conditioned overnight (20 ± 2 °C, 65 ± 2 % relative humidity) and its average linear density (tex = g/1000m) value was calculated from a 5 m hank of yarn prior to the measurement. The fabric's resistance to staining has been assessed by adapting a respective procedure for the plastic materials according to NEMA LD 3-2005 and textile fabrics according to ASTM D1308. In general terms, each fabric sample measuring 50 × 50 mm was placed on the non-porous surface and two drops of each staining agent (tomato ketchup, plain prepared yellow mustard, freshly prepared coffee, red wine and corn oil) were deposited for 60 min at 25 °C. After that the sample was treated for six washing operations without rubbing followed by drying at 40 °C in a ventilated oven: (i) cold water-flush removal (if the stain disappears, score 0); (ii) cold water flush washing with non-ionic detergent (if the stain disappears, score 1); (iii) cold water washing using hand-washing commercial detergent (if the stain disappears, score 2); (iv) 30 °C washing using commercial detergent (if the stain disappears, score 3) (v) spotting remover with a solvent-based cleaner (if the stain disappears, score 4) and (vi) washing with a water-bleach detergent solution (perborate) (if the stain disappears, score 5). Final cleanability is the sum of the scores from all staining agents, where 0 is the best score and 25 is the worst score.

3. Results and discussion

3.1. Fibre spinning

Depolymerised suberin (SUB) represents a mixture of hydroxy fatty acids and dicarboxylic acids, the most abundant being 18-hydroxyoctadec-9-enoic, 9,10-epoxy-18-hydroxyoctadecanoic, 9,10,18-trihydroxyoctadecanoic and 22-hydroxydocosanoic acids (Table S1, Supplementary data). In turn, the predominant components of the cutin fraction (CUT) were triterpenoids, the predominant being oleanolic acid (almost 60 %), followed by waxy material (ca. 20-30 %) (Table S2, Supplementary data), whose composition was suggested to be a mixture of fatty acid esters of fatty alcohols (e.g., hexacosanol, octacosanol, tetracosanol and triacosanol) (Mendes et al. 2013a). The colour of the samples obtained by modification with SUB (dark brown) and CUT (green) is noteworthy. According to previous findings related to the structure relationship of the hydrophobic agent and its compatibility with Ioncell fibres regenerated from dope, the presence of polar groups (e.g., carboxyl groups) in hydrophobic additives favours their retention and more homogeneous distribution on the fibre surface (Moriam et al. 2021). Thus, betulinic acid showed better performance than structurally parent betulin both in terms of spinnability and fibre coating. Hence, both SUB and CUT additives possessing carboxyl groups and hydrophobic tail could be considered as good candidates for the hydrophobisation of Ioncell fibres.

The addition of less than 10 % (w/w) of hydrophobisation agent (e.g., triterpenoids or lignin) to the dope could not be sufficient to obtain regenerated ioncell fibres with hydrophobic properties (Moriam et al. 2021). Accordingly, the loads of SUB and CUT were adjusted to approximately 10 % (w/w). Taking into consideration the maximum solubility of cellulose in [DBNH][OAc] ionic liquid (about 13 %, w/w) (Sixta et al. 2015), the introduction of ca 10 % (w/w) SUB and CUT had to decrease the cellulose content to ca 11.7 % maintaining the similar load of dope ingredients for comparison reasons (ca 13 %). Unlike the control dope with cellulosic fibres only (dissolving pulp) possessing yellowish colour, the dopes with SUB and CUR were stronger coloured exhibiting brownish colour with SUB and greenish colour with CUT. The typical images of prepared dope before and after the filtration stages are shown in Fig. 1.

Similarly to previous assays with addition of betulin and betulinic acid in the dope (Moriam et al. 2021), the addition of SUB and CUT led to the increased complex viscosity (η*) and to the decreased dynamic modulus due to the less content of cellulose in solution when compared to the control assay without additive. In all experiments the cellulose solutions with additives did not exceed the recommended optimum spinning [η_0] window for cellulose solution in [DBNH][OAc] of 20000−30000 Pa·s (Michud et al. 2016a; 2016b) that allowed to operate with the desired drawing ratio (DR) of 14-18 to attain comparable fibre linear density of ~1.3 dtex. The colour of span regenerated fibres varied from colourless of additive-free fibres to aureate and silvery of SUB and CUT added fibres, respectively (Fig. 1). The regenerated fibres had a round and smooth surface.

The evaluation of a real additive uptake on the Ioncell fibres was carried out by their exhaustive Soxhlet extraction. A significant difference was found between SUB and CUT additives concerning their retention on the regenerated Ioncell fibres, which was 2.5 % and 8.5 % (w/w), respectively (Fig. 2). Thus, a clear discrimination was observed in SUB retention, whereas CUT retention was similar to that previously reported for betulinic acid in the same experimental set (Moriam et al. 2021). The main reason is the greater hydrophilicity of the hydroxy fatty acids in SUB compared to oleanolic acid and waxes in CUT and their easier removal in an aqueous precipitation bath and in washing to remove residual ionic liquid. In fact, the contact angle with water of SUB film varied between 105 and 115°, whereas the CUT film varied in the range of 130-140°.

3.2. Physical properties of modified fibres

3.2.1. Strength properties

At the similar linear density of unmodified (ICF) and modified Ioncell fibres, the latter ones showed lower tenacity (Table 1). This was especially noticeable for the SUB modified fibres (ICFSUB) and much less for the CUT modified fibres (ICFCUT). These differences must be due to less oriented cellulose fibrils in ICFSUB and ICFCUT than in ICF, as revealed by birefringence analysis (Table 1). Furthermore, not only does the crystalline orientation play an important role in the deformation behaviour of the regenerated fibres, but also the orientation of the amorphous phase and the occurring voids are equally important (Asaadi et al. 2018). However, orientation is not the only factor that affected the decline in ICFSUB's tenacity, because these indicators were not coherent in the case of ICFSUB and ISFCUT. WAXS analysis showed the lowest degree of crystallinity and average width of cellulose crystallites in ICFSUB (Table 1, Fig 3), the last being ca 17 % lower than that for ICF and ca 7 % lower than for ICFCUT. As the strength characteristics of the regenerated fibres are affected by the cross dimensions of the crystallite (Sawada et al. 2021), the coherence between the D_{110} values and the tenacity of the Ioncell fibres pointed to an important positive relationship between them. Hence, the addition of SUB in dope provided worst

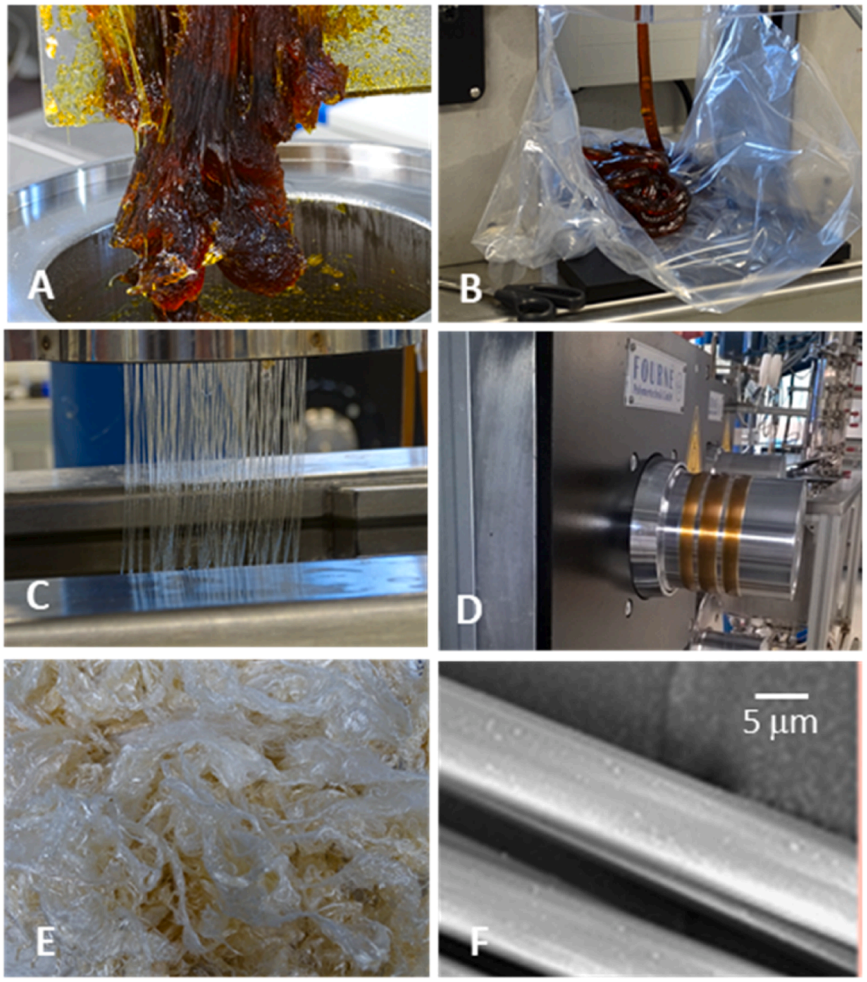

Fig. 1. Overview of a cellulose solution in [DBNH][OAc] (dope) with the addition of 10 % (w/w) depolymerised suberin (SUB) before (A) and after filtration (B); the extrusion of the dope in the coagulation water bath (C) led to the formation of regenerated fibres which, after spinning, accumulated on the roll (D). The washed cut fibres (E) were further opened using a fibre opener. Ioncell fibres possessed a smooth surface (F), as revealed by SEM microscopy.

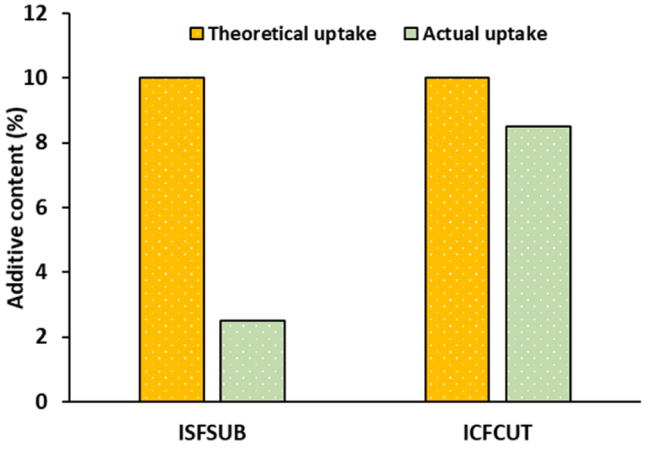

Fig. 2. Theoretical and actual uptake of depolymerised suberin (SUB) and a cutin fraction (CUT) on the Ioncell fibres (ICFSUB and ICFCUT).

conditions for the cellulose fibril spatial organisation and orientation during coagulation and spinning steps.

3.2.2. *Surface properties*

Surface properties were assessed by measuring contact angles with water on the non-woven fabrics (fibre sheets) produced from unmodified and modified Ioncell fibres. Both ICFSUB and ICFCUT revealed a significant increase in fibre hydrophobicity after modification, being the most pronounced for ICFCUT showing a contact angle almost 101° (Table 2). This fact must be related to higher additive uptake in ICFCUT than in ICFSUB (Fig. 2). The surface composition of the modified fibres confirmed a relative increase in total carbon content (C1s) with a simultaneous increase in non-oxygenated carbons (CC) and a decrease in oxygenated carbons (CO) (Table 2). This was particularly notable in ICFCUT, which can be explained by its higher carbon content and higher fibre absorption.

The presence of SUB and CUT on the fibre surface was confirmed by FTIR-ATR spectra (Fig. 4). Although the spectra difference between reference fibres (ICF) and fibres modified with SUB was minor, the difference between the ICF and fibres modified with CUT was quite notable. Thus, were detected the characteristic for oleanolic acid signals from carboxyl groups (C=O stretching in COOH at 1716 cm^{-1}) and from methylene and methyl moieties (C-H stretching at 2918 cm^{-1} and 2852 cm^{-1}). A relatively low uptake of SUB in Ioncell fibres (Fig. 2) may explain the little difference between its spectrum and the spectrum of the original ICF fibres (Fig. 4). As FTIR-ATR spectra characterize only the surface of the analysed material, these data indicate the allocation of SUB and CUT additives outside the modified fibres.

The presence of hydrophobic additives on the external surface of modified Ioncell fibres was additionally confirmed by AFM operated in a tapping mode (Fig. 5). This was particularly notable for CUT modified

Table 1
Strength properties of unmodified (ICF) and modified (ICFSUB and ICFCUT) Ioncell fibres, their average crystallite widths in 110 plane (D_{110}) and crystalynity index (*CrI*).

Fibre sample	Fibre mechanical properties (conditioned)					D_{110} (nm)	CrI
	Linear density (dtex)	Tenacity (cN/tex)	Elongation (%)	Birefringence			
				Δn	f_t		
ICF	1.30 ± 0.16	46.83 ± 2.02	12.52 ± 1.49	0.044 ± 0.010	0.704 ± 0.16	3.42	0.65 ± 0.01
ICFSUB	1.32 ± 0.09	38.69 ± 1.18	9.79 ± 0.67	0.039 ± 0.004	0.632 ± 0.067	2.85	0.62 ± 0.01
ICFCUT	1.33 ± 0.14	41.15 ± 2.54	9.89 ± 1.15	0.034 ± 0.005	0.543 ± 0.087	3.06	0.64 ± 0.01

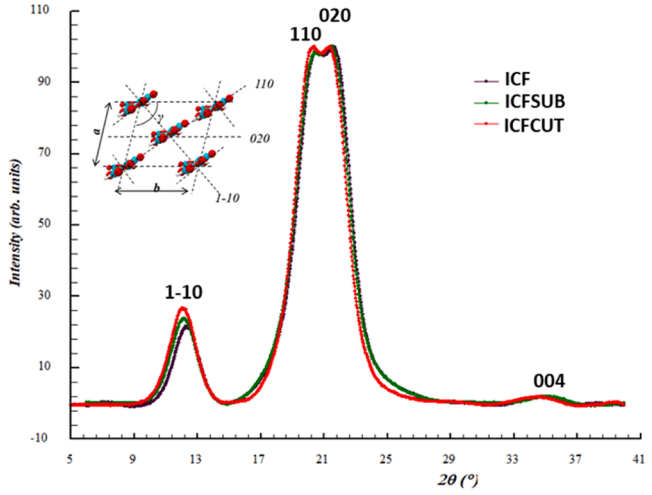

Fig. 3. WAXS diffraction patterns of pristine Ioncell fibres (ICF) and those modified by depolymerized suberin (ICFSUB) and a cutin fraction (ICFCUT). The lattice planes are represented in the elementary cellular projection of the cellulose II polymorph.

Table 2
Surface chemical composition of unmodified (ICF) and modified (ICFSUB and ICFCUT) Ioncell fibres as revealed by XPS analysis and their contact angle with water (WCA).

Fibre sample	Atomic percentage from wide scan XPS analysis (%)					WCA in non-woven (deg.)
	C1s	O1s	N1s	CC	CO	
ICF	77.2	19.7	0.4	55.4	32.5	64.2 ± 5.2
ICFSUB	77.5	21.1	0.3	54.7	31.7	95.1 ± 2.0
ICFCUT	78.4	18.7	0.5	56.4	29.5	100.8 ± 3.5

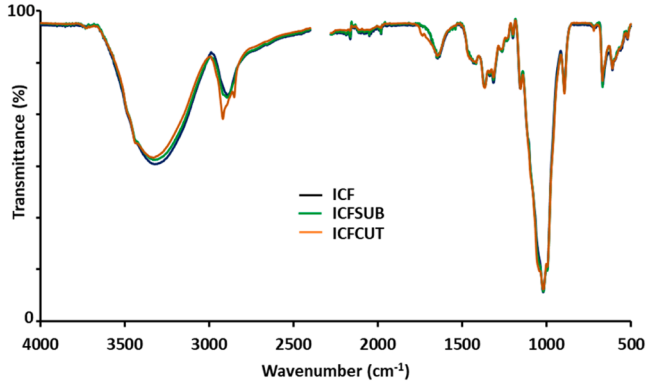

Fig. 4. Normalised FTIR-ATR spectra of pristine Ioncell fibres (ICF) and those modified by depolymerised suberin (ICFSUB) and a cutin fraction (ICFCUT).

fibres due to the relatively high abundance of this hydrophobisation agent. Thus, the surface of ICFCUT fibres was remarkably rougher (S_a = 6.2 ± 1.3 nm) compared to the unmodified ICF fibres (S_a = 3.7 ± 1.4 nm). The images acquired in an amplitude modulation mode for ICF and ICFCUT show higher similarity (Fig. 5 A, B). However, the phase imaging mode allowed clearly distinguish the stiffer cellulosic fibrils and softer CUT deposited on the fibre surface (Fig. 5 C, D). According to these images, CUT must have an irregular distribution on the Ioncell fibres, thus forming discontinuous coverage with apparently isolated spots. The irregular coverage of the fibre may be due to the fact that CUT and SUB tend to aggregate, thus showing better internal affinity than affinity with cellulose fibre. This fact can explain a lower detected contact angle (ca 101°) that could be expected if CUT covered all fibre surface (130-140°). Similar features were suggested previously for the deposition of betulinic acid on the regenerated Ioncell fibres carried out under similar conditions (Moriam et al., 2021).

The distribution of the CUT in the Ioncell fibres was also assessed by confocal Raman spectroscopy (Fig. 6). For this, ICFCUT Ioncell fibres were embedded in the acrylic resin (LR White) and, after curing, cut perpendicularly into thin slices of ca. 2 μm thick and submitted to Raman imaging analysis.

In Fig. 6A, the area marked in red corresponds to the optical microscopy image of the ICFCUT fibres embedded into the soft acrylic resin and the corresponding combined Raman image is shown on the right panel. A total of 40000 Raman spectra (200 points x 200 lines) were collected across the resin area (100 μm x 100 μm) to generate the Raman map presented in Fig. 6B, which shows the presence of Ioncell fibres (blue colour) and CUT extract (green colour) on the acrylic resin (red colour). The Raman spectrum of the acrylic resin (red spectrum, Fig. 6C) shows the characteristic bands of LR White resin: 2950 cm^{-1}, ν_{asym}(C-H_3); 2895 cm^{-1}, ν_{sym}(C-H_3); 1724 cm^{-1}, ν(C=O); 1648 cm^{-1}, ν(C=C) and ν(C-COO); 1460 cm^{-1}, δ(C-H_3) and δ(O-CH_3); 1100 cm^{-1}, CH_3 twisting mode; 975 cm^{-1}, ν(C-C); 850 cm^{-1}, CH_2 rocking mode. The Raman spectrum depicted in blue (Fig. 6C) is due to the presence of Ioncell fibres, showing the characteristic bands of cellulose: 2892 cm^{-1}, ν(C-H_3); 1479 cm^{-1}, δ(H-C-H); 1377 cm^{-1}, δ(H-O-C); 1094 cm^{-1}, ν(C-H), ν(C-H_2) and ν_{asym}(C-O-C) glycosidic linkage. Despite the grape skin extract (CUT) did not show any strong Raman bands, only fluorescence (green spectrum, Fig. 6C), this feature can be monitored by Raman imaging. This result clearly shows that CUT extract is mainly distributed on the surface of the modified fibres, confirming the result previously obtained by AFM. Although the hydrophobic agent (CUT) was detected practically exclusively on the fibre surface, some minor visible inclusions inside fibrils were also observed. These can be both real inclusions inside fibres, but also false spots that appeared during the sample cutting while the CUT from the outside was smeared over the cut surface.

3.2.3. Water vapour sorption

The response to the water sorption of unmodified and modified Ioncell fibres revealed hydrophobisation effect of SUB and CUT being increased in the order ICF-ICFSUB-ICFCUT (Fig. 7). This is in tune with the increase of the surface hydrophobicity detected for the modified fibres (Table 2). The application of the GAB model allowed the

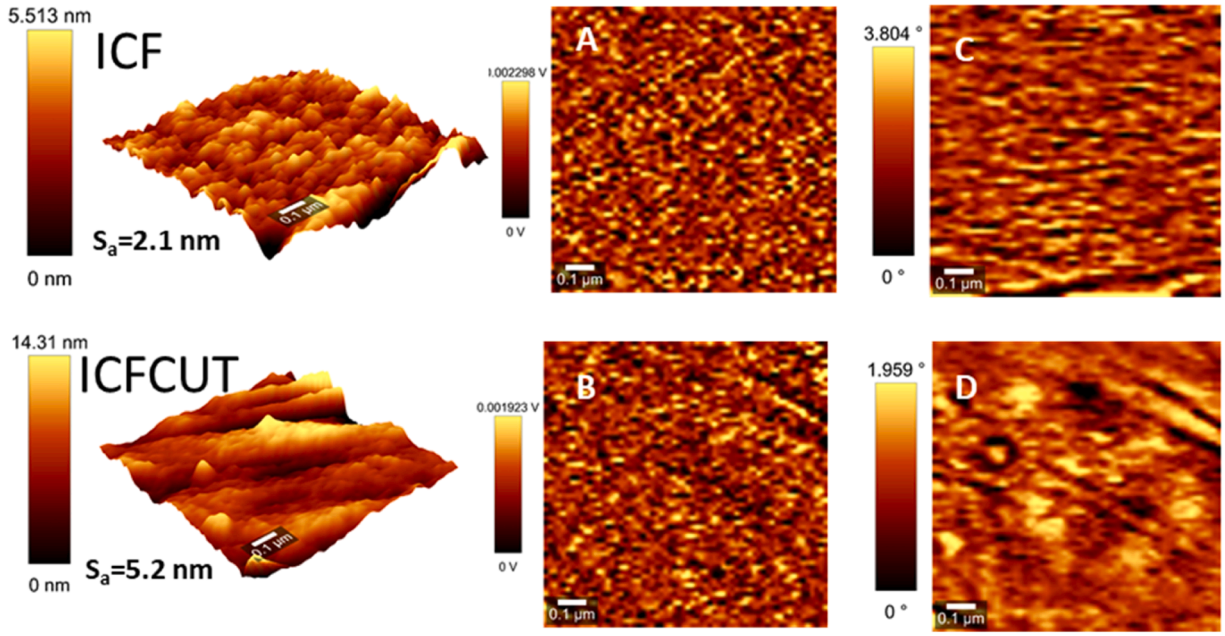

Fig. 5. AFM images of the surface of pristine Ioncell fibres (ICF) and those modified by a cutin fraction (ICFCUT) acquired in a taping mode. The respective images acquired in amplitude modulation mode (A and B) and phase imaging mode (C and D) are shown on the right side.

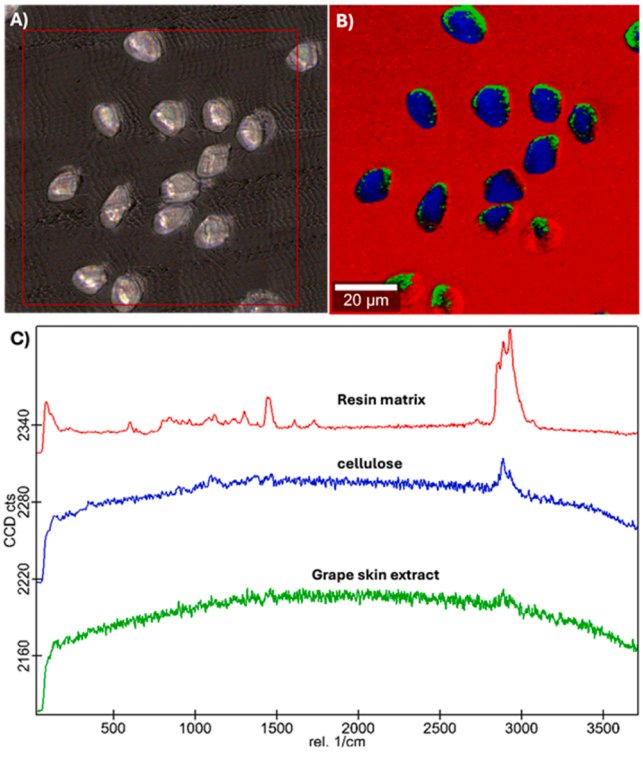

Fig. 6. A) Optical microscopy image of transversal cut of ICFCUT fibres embedded into the soft acrylic resin. B) Raman image obtained by the combination of the three distinct Raman spectra. C) Raman spectra used for the combined Raman image: acrylic resin (red), Ioncell fibre (blue) and CUT extract (green). combination of specific fluorescence zones from the Ioncell fibres (blue colour) coated by cutin fraction (green colour) embedded in the matrix resin (red colour).

evaluation of monolayer capacity (X_m) and energetic parameters of water sorption in monolayer (C) and in multilayer (K) as well as changes in specific surface of fibres (Table 3). The referred parameters were

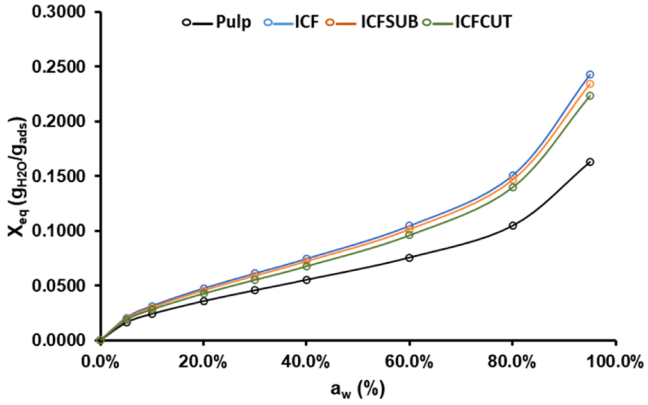

Fig. 7. Sorption isotherms (25 °C) of the dissolving pulp (Pulp) and the Ioncell fibres produced thereof: pridtine fibres (ISF) and those modified by depolymerised suberin (ICFSUB) and cutin fraction (ICFCUT).

Table 3
Effective parameters of the GAB model of water vapour sorption by unmodified (ICF) and modified (ICFSUB and ICFCUT) Ioncell fibres (25 °C).

Fibre sample	$X_m \pm dX_m$ (g_{H2O}/g)	C ± dC (dimensionless)	K ± dK (dimensionless)	S (m^2/g)	Fraction of the occupied sites in the monolayer (ζ*)
Pulp	0.048 ± 0.003	10.90 ± 0.79	0.71 ± 0.06	202 ± 8	0.96
ICF	0.064 ± 0.003	10.01 ± 0,38	0.76 ± 0,05	267 ± 10	0.97
ICFSUB	0.062 ± 0,003	9.63 ± 0,31	0.76 ± 0,05	259 ± 7	0.97
ICFCUT	0.058 ± 0,003	9.61 ± 0,40	0.77 ± 0,05	241 ± 8	0.95

*$\zeta = C \cdot K \cdot a_w/(1+(C-1) \cdot K \cdot a_w)$.

compared with those of parent dissolving pulp used to produce Ioncell fibres.

As expected, the Ioncell fibres showed higher monolayer capacity X_m and specific surface area S than the original soluble cellulose fibres due to the less ordered cellulose structure of the former (Ciechańska et al. 2009; Klemm et al. 1998). Besides lower crystallinity of the regenerated cellulose, the detected average width of cellulose II crystallites in Ioncell fibres (ca. 3 nm, Table 1) was inferior to those typically detected for cellulose I in sulphite pulp fibres (4-5 nm) (Rebuzzi and Evtuguin, 2005) thus promoting additionally the higher accessible area. The X_m of modified Ioncell fibres decreased from 3 % in SUB modified to almost 10 % in CUT modified fibres with simultaneous decrease in the specific accessible area (Table 3). All this decrease in X_m and S can be explained by partial surface coverage of fibres by SUB or CUT thus restricting the access of water molecules. At the same time, the detected lower sorption enthalpy in the monolayer of modified fibres related to the C parameter also indicates the eventual impediment of water interaction with accessible cellulose hydroxyl groups in the presence of hydrophobic additives. One of the possible reasons could be limited swelling due to difficulty in penetrating water inside the fibres. As no significant changes were detected in the parameter K related to sorption enthalpy in multilayers, it can be suggested that the surface potential of the fibrils did not change significantly upon fibre modification.

3.3. Enzymatic hydrolysis

Rayon fibres are more sensitive to mildew and mould than cotton fibres and this is one of the weaknesses of the former (Cook 2001; Sanders et al., 2021; Sular and Devrim, 2019; Szostak-Kotowa 2004). Microbiological attack generally results in weakening of fibre strength due to partial enzymatic hydrolysis by extracellular enzymes (mainly cellulases). In this context, the effect of modifying Ioncell fibre with SUB and CUT on enzymatic hydrolysis by endo-cellulase was evaluated.

The comparison of reducing sugars release in the reaction with commercial endo-cellulase demonstrated different dynamics of unmodified (ICF) and modified Ioncell fibres, ICFSUB and ISFCUT (Fig. 8). Thus, for unmodified fibres, a first rapid hydrolysis step over a period of 5 to 25 min was followed by a relatively slow hydrolysis over the next 25 to 90 min and then accelerates again to reaction time as long as 90 min. The first step corresponds to the hydrolysis from the readily accessible fibre surface and is predetermined by the rate of enzymatic hydrolysis. The second step depends on the enzyme diffusion in the interior of fibre structure and the last step is auto accelerative due to the steady increased enzymatic accessibility in hydrolysed fibre cavities and improved fibre swelling.

Modified Ioncell fibres clearly showed decreased enzyme accessibility and slower enzyme diffusion within the fibres (Fig. 8). This was particularly notable for the CUT modified fibres (ICFCUT), which revealed almost three times smaller initial hydrolysis rate than unmodified fibres. The role of SUB and CUT may not only be to prevent enzymatic attack on the fibre surface due to the isolation effect, but also due to their hydrophobicity, affecting the penetration of water into the fibres, thus hindering their swelling. Accordingly, it can be suggested that SUB or CUT modified Ioncell fibres should be more resistant to mildew and mould action that the parent ICF. Taken into consideration also the known antiviral and antibacterial properties of triterpenic acids (Dzubak et al., 2006; Perumal and Dharmarajan, 2005), the main component of CUT (Table S2, Supplementary Data), it can be proposed that at least ICFCUT should also have antimicrobial properties. However, this point needs further experimental confirmation.

3.4. Yarn spinning

The produced staple fibres were prepared for yarn spinning by washing with water, air drying and opening with a fibre opener. The spin-finish treatment was not applied before spinning the yarn to avoid

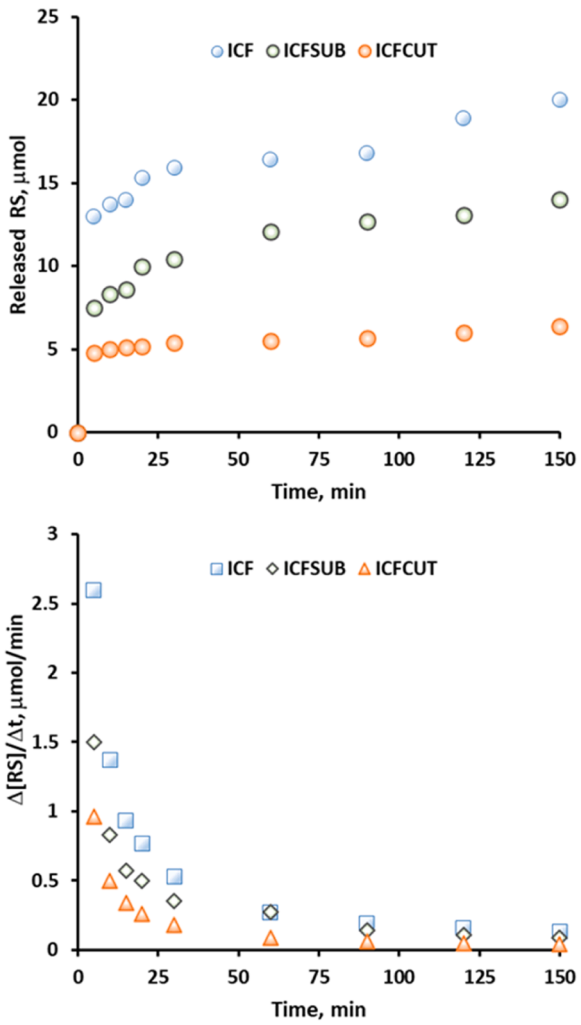

Fig. 8. Integral (upper figure) and differential (lower figure) curves of enzymatic hydrolysis of pristine Ioncell fibres (ISF) and those modified by depolymerised suberin (ICFSUB) and cutin fraction (ICFCUT).

losses of modifying agents (SUB and CUT). This fact can explain some heterogeneity in the sliver, resulting in a greater standard deviation of the linear densities and tensile properties of the yarn (Table 4). Tensile properties of yarns produced from modified Ioncell fibres (ICFSUB and ICFCUT) were roughly 20 % inferior to those obtained for the unmodified fibres (ICF) maintaining similar elongation at break. This can be attributed, at least partially, to some lower strength of the modified fibre compared to the unmodified fibres (Table 1). However, the yarn structure also contributes significantly to its tensile properties (Klein, 1986). In particular, the twist angle (or twist density) affects the yarn tensile properties reaching some optimum level, which was apparently not attained in this study.

The strength realisation in the yarn, expressed as the ratio of the mean yarn tenacity to the mean fibre tenacity for the ICF, and ISFSUB and ISBCUT yarns were 58 % and 48 %, respectively. Similar values are recently reported for the unmodified Ioncell fibres and fibres modified

Table 4
Strength properties of yarns produced from pristine Ioncell fibres (ICF) and depolymerised suberin (ICFSUB) or cutin fraction (ICFCUT) modified fibres.

Sample	Linear density (tex)	Tenacity (cN/tex)	Elongation (%)
ICF yarn	22.9 ± 2.2	26.9 ± 4.8	7.6 ± 0.7
ICFSUB yarn	20.2 ± 3.1	18.6 ± 5.2	6.3 ± 1.6
ICFCUT yarn	20.1 ± 2.9	19.8 ± 6.5	6.5 ± 0.8

by betulinic hydrophobic agents (Moriam et al., 2021). The tensile strength of either ISFSUB and ISBCUT yarns, for the comparable linear density (ca 20-30 tex), were superior to those commonly reported for the viscose (Mendes et al. 2021; Michud et al., 2016a).

3.5. Staining resistance of Ioncell fabrics

Knitted/handloomed fabrics were prepared for demonstration purposes. All fabrics produced were similar in colour to the respective unmodified and modified Ioncell fibres and similar in feel to the touch. Similar features were also noticed for the respective nonwovens (Fig. S1, Supplementary data). The fabrics produced with unmodified fibres (ICF) absorbed water drop within less than 1 s, whereas fabrics produced from SUB and CUT modified fibres within ca. 2 and 6 s, respectively, thus confirming the remaining hydrophobicity. Fabrics with hydrophobic properties are commonly associated with dirt repellent capacities. These were assessed using an adapted test for the staining resistance using five staining substances (tomato ketchup, plain prepared yellow mustard, freshly prepared coffee, red wine and corn oil) and measuring the appearance score (0-25 scale) after five preselected washing operations.

The results are summarised in Table 5. The modification of Ioncell fibres either with SUB or CUT allowed the improvement of the cleanability of respective fabrics, which was more pronounced for those produced from fibres modified with CUT (lowest score). This can be explained by the highest CUT uptake in the Ioncell fibres and the better surface hydrophobicity provided. Noteworthy that the hydrophobic properties of modified fibres were lost almost completely after the washing with commercial detergents though the hydrophobic properties of Ioncell fibres modified with CUT were maintained after washing with hot water (70-90 °C) only.

Table 5
Results on the cleanability of knitted fabrics produced from unmodified (ICF) and modified Ioncell fibres modified by depolymerised suberin (ICFSUB) or cutin fraction (ICFCUT).

Staining agent	Cleanability (appearance scoring)		
	ICF fabric	ICFSUB fabric	ICFCUT fabric
Ketchup	5	4	3
Mustard	3	3	2
Coffee	4	3	3
Red wine	5	4	3
Corn oil	3	2	1
Total score	20	16	12

4. Conclusions

The results of this study demonstrated a promising potential of added in dope depolymerised suberin compounds (SUB) or cutin fraction extractable by dichloromethane from grape skins (CUT) for imparting hydrophobic properties to regenerated cellulosic fibres obtained by Ioncell-F® method. The superior retention in regenerated Ioncell fibres and the greater hydrophobic effect of CUT compared to SUB are explained by differences in their composition, where CUT contains little polar triterpenoids and waxes, instead of more polar hydroxy fatty acids and dicarboxylic acids present in SUB. Hence, hydrophobising additive retention in the regenerated fibres depended on its polarity and water affinity in a coagulation bath, being more favourable for CUT than for SUB. More hydrophobic and better retained on the fibre CUT (more than triple to SUB) allowed to achieve a higher contact angle with water in nonwovens than less hydrophobic and less retained on the fibre SUB (ca. 101° versus ca. 95°). When hydrophobic additives are added to the extruded dope, they do not deteriorate spinning and are irregularly distributed essentially on the surface of regenerated fibres. However, the addition of hydrophobising additives in dope decrease slightly (ca. 10-20 %) the tensile strength of regenerated modified fibres due to the less favourable conditions for the cellulose fibril spatial organisation and orientation during coagulation and spinning steps. The hydrophobising additives in study provide to regenerated modified fibres better waterproof performance when compared to pristine Ioncell fibres and a higher resistance to enzymatic hydrolysis with cellulase suggesting they may be less susceptible to microbial degradation. Knitted fabrics produced from modified hydrophobized Ioncell fibres demonstrated much better dirt repellence and cleanability than those produced from pristine Ioncell fibres.

The eventual loss in hydrophobic properties that happened in spin-finish treatment during yarn production and in washing of woven fabrics with commercial detergents can be diminished by previous treatment of modified regenerated fibres using appropriate chemical, biochemical or physical methods. At the same time, the detected loss in hydrophobicity during washing operations with detergents is not a limiting factor for non-woven tissues for industrial or agricultural applications.

CRediT authorship contribution statement

Kaniz Moriam: Writing – original draft, Visualization, Methodology, Investigation. **Catarina Azevedo:** Writing – review & editing, Methodology, Investigation. **Sara Fateixa:** Writing – review & editing, Methodology, Investigation. **Fábio Bernardo:** Writing – review & editing, Methodology, Investigation. **Herbert Sixta:** Writing – review & editing, Supervision, Project administration, Methodology, Conceptualization. **Dmitry V. Evtuguin:** Writing – review & editing, Validation, Supervision, Methodology, Funding acquisition, Conceptualization.

Declaration of competing interest

The authors declare that they have no known competing financial interests or personal relationships that could have appeared to influence the work reported in this paper.

Acknowledgements

The financial support of this work by Caima – Indústria de Celulose S. A. and by project CICECO-Aveiro Institute of Materials, UIDB/50011/2020 (DOI 10.54499/UIDB/50011/2020), UIDP/50011/2020 (DOI 10.54499/UIDP/50011/2020) & LA/P/0006/2020 (DOI 10.54499/LA/P/0006/2020), financed by national funds through the FCT/MCTES (PIDDAC). This was also done within the scope of Finland Academy project (under the project WTF-Click-Nano), Tekniikan Edistämissäätiö, Finnish Cultural Foundation, Puunjalostus Insinöörit, Walter Ahlström Foundation and Jenny and Antti Wihuri grant foundation. Dr. Sara Fateixa thanks FCT for research contract funded by National funds (OE), in the scope of the framework contract foreseen in the numbers 4, 5, and 6 of article 23, of the Decree-Law 57/2016, of August 29, changed by Law 57/2017, of July 19 (DOI 10.54499/DL57/2016/CP1482/CT0007). The authors also gratefully acknowledge Nicole Nygren (Aalto University) for her support in fibre testing; Simone Haslinger and Leena Katajainen for their help during fibre spinning; Azovskaya Valeriya (Aalto university) for assisting in image/photo preparation; students from Aveiro University Teodora Silva, Adriana Correia and Liliana Lameiras for their help in producing suberin and cutin-modified fibres.

Supplementary materials

Supplementary material associated with this article can be found, in the online version, at doi:10.1016/j.carpta.2024.100613.

Data availability

Data will be made available on request.

References

Asaadi, S., Hummel, M., Ahvenainen, P., Gubitosi, M., Olsson, U., & Sixta, H. (2018). Structural analysis of Ioncell-F fibres from birch wood. *Carbohydrate Polymers, 181*, 893–901. https://doi.org/10.1016/j.carbpol.2017.11.062

Asaadi, S., Hummel, M., Hellsten, S., Härkäsalmi, T., Ma, Y., Michud, A., & Sixta, H. (2016). Renewable high-performance fibers from the chemical recycling of cotton waste utilizing an ionic liquid. *ChemSusChem, 9*(22), 3250–3258. https://doi.org/10.1002/cssc.201600680

Björquist, S., Aronsson, J., Henriksson, G., & Persson, A. (2018). Textile qualities of regenerated cellulose fibers from cotton waste pulp. *Textile Research Journal, 88*(21), 2485–2492. https://doi.org/10.1177/0040517517723021

Branco, D., Campos, J. R., Cabrita, L., & Evtuguin, D. V. (2020). Structural features of macromolecular components of cork from *Quercus suber* L. *Holzforschung, 74*(6), 625–633. https://doi.org/10.1515/hf-2019-0271

Ciechańska, D., Wesolowska, E., & Wawro, D. (2009). An introduction to cellulosic fibres. In S. J. Eichhorn, J. W. S. Hearle, M. Jaffe, & T. Kikutani (Eds.), *Handbook of textile fibre structure. Volume 2: Natural, regenerated, inorganic and specialist fibres* (1st ed., pp. 3–61). Woodhead Publishing Limited. https://doi.org/10.2115/fiber.66.P_174. Vol. 66, Issue 5.

Cook, J. G. (2001). *Handbook of textile fibres. II. Man-made fibres* (5th ed.). Sawston, UK: Woodhead Publishing Ltd.

Correia, V. G., Bento, A., Pais, J., Rodrigues, R., Haliński, Ł. P., Frydrych, M., Greenhalgh, A., Stepnowski, P., Vollrath, F., King, A. W. T., & Silva Pereira, C. (2020). The molecular structure and multifunctionality of the cryptic plant polymer suberin. *Materials Today Bio, 5*, Article 100039. https://doi.org/10.1016/j.mtbio.2019.100039

Dzubak, P., Hajduch, M., Vydra, D., Hustova, A., Kvasnica, M., Biedermann, D., Markova, L., Urban, M., & Sarek, J. (2006). Pharmacological activities of natural triterpenoids and their therapeutic implications. *Natural Product Reports, 23*, 394–411. https://doi.org/10.1039/b515312n

Edgar, K. J., & Zhang, H. (2020). Antibacterial modification of Lyocell fiber: A review. *Carbohydrate Polymers, 250*, Article 116932. https://doi.org/10.1016/j.carbpol.2020.116932

Elsayed, S., Hummel, M., Sawada, D., Guizani, C., Rissanen, M., & Sixta, H. (2021). Superbase-based protic ionic liquids for cellulose filament spinning. *Cellulose, 28*(1), 533–547. https://doi.org/10.1007/s10570-020-03505-y

Ferreira, A. R. F. C., Figueiredo, A. B., Evtuguin, D. V., & Saraiva, J. A. (2011). High pressure pre-treatments promote higher rate and degree of enzymatic hydrolysis of cellulose. *Green Chemistry : An International Journal and Green Chemistry Resource : GC, 13*, 2764–2767. https://doi.org/10.1039/C1GC15500H

Ferrero, F., & Periolatto, M. (2013). Application of fluorinated compounds to cotton fabrics via sol–gel. *Applied Surface Science, 275*, 201–207. https://doi.org/10.1016/j.apsusc.2013.01.001, 2013.

Fink, H.-P., Weigel, P., Purz, H. J., & Ganster, J. (2001). Structure formation of regenerated cellulose materials from NMMO-solutions. *Progress in Polymer Science, 26*(9), 1473–1524. https://doi.org/10.1016/S0079-6700(01)00025-9

Firgo, H., Eibl, M., & Eichinger, D. (1996). Lyocell - Eine ökologische Alternative. *Lenzinger Berichte, 75*, 47–50.

Food and Agriculture Organization of the United Nations. (2022). *Forestry production and trade*. http://www.fao.org/faostat/en/#data/FO.

Forsman, N., Johansson, L.-S., Koivula, H., Tuure, M., Kääriäinen, P., & Österberg, M. (2020). Open coating with natural wax particles enables scalable, non-toxic hydrophobation of cellulose-based textiles. *Carbohydrate Polymers, 227*, Article 115363.

Heredia, A. (2003). Biophysical and biochemical characteristics of cutin, a plant barrier biopolymer. *Biochimica et Biophysica Acta, 1620*(1), 1–7. https://doi.org/10.1016/s0304-4165(02)00510-x

Huang, T., Chen, C., Li, D., & Ek, M. (2019). Hydrophobic and antibacterial textile fibres prepared by covalently attaching betulin to cellulose. *Cellulose, 26*(1), 665–677. https://doi.org/10.1007/s10570-019-02265-8

Huang, T., Li, D., & Ek, M. (2018). Water repellency improvement of cellulosic textile fibers by betulin and a betulin-based copolymer. *Cellulose, 25*(3), 2115–2128. https://doi.org/10.1007/s10570-018-1695-5

Hummel, M., Michud, A., Tanttu, M., Asaadi, S., Ma, Y., Hauru, L. K. J., Parviainen, A., King, A. W. T., Kilpeläinen, I., & Sixta, H. (2016). Ionic liquids for the production of man-made cellulosic fibers: opportunities and challenges. In O. J. Rojas (Ed.), *Advances in polymer science* (1st ed., pp. 133–168). Springer International Publishing. https://doi.org/10.1007/978-3-319-26015-0. Vol. 271.

Klein, W. (1986). The technology of short-staple spinning. In H Stalder (Ed.), *Manual of textile technology* (2nd Edition). Manchester, UK: Textile Institute.

Klemm, D., Philipp, B., Heinze, T., Heinze, U., & Wagenknecht, W. (1998). Comprehensive cellulose chemistry: Volume I: Fundamentals and analytical methods. *Methods (San Diego, Calif.)* (Vol. l,, 260. https://doi.org/10.1002/3527601929

Lenz, J., Schurz, J., & Wrentschur, E. (1994). On the elongation mechanism of regenerated cellulose fibres. *Holzforschung, 48*(s1), 72–76.

Li-Beisson, Y.; Verdier, G.; Xu, L. and Beisson, F. (2016) Cutin and suberin polyesters. In: eLS. John Wiley &Sons, Ltd: Chichester, United Kindom. https://doi.org/10.1002/9780470015902.a0001920.pub3.

Ma, Y., Asaadi, S., Johansson, L.-S., Ahvenainen, P., Reza, M., Alekhina, M., … Sixta, H. (2015). High strength composite fibres from cellulose-lignin blends regenerated from ionic liquid solution. *ChemSusChem, 8*(23), 4030–4039. https://doi.org/10.1002/cssc.201501094

Makarov, I., Vinogradov, M., Gromovykh, T., Lutsenko, S., Feldman, N., Gulbarshin Shambilova, G., & Sadykova, V. (2018). Antifungal composite fibers based on cellulose and betulin. *Fibers, 6*(2), 23. https://doi.org/10.3390/fib6020023

Mendal, N., Sahito, I. A., Arbab, A. A., Sun, K. C., Qadir, M. B., Memon, A. A., & Jeong, S. H. (2016). Fabrication of a flexible and conductive lyocell fabric decorated with graphene nanosheets as a stable electrode material. *Carbohydrate Polymers, 152*, 19–25. https://doi.org/10.1016/j.carbpol.2016.06.099

Mendes, I. S. F., Prates, A., & Evtuguin, D. V. (2021). Production of rayon fibres from cellulosic pulps: State of the art and current developments. *Carbohydrate Polymers, 273*, Article 118466. https://doi.org/10.1016/j.carbpol.2021.118466

Mendes, J. A. S., Evtuguin, D. V., & Cruz Lopes, L. P. (2013a). Towards comprehensive utilization of winemaking residues: Characterization of grape skins from red grape pomaces of variety Touriga Nacional. *Industrial Crops and Products, 43*, 25–32.

Mendes, J. A. S., Xavier, A. M. R. B., Evtuguin, D. V., & Cruz Lopes, L. P. (2013b). Integrated utilization of grape skins from white grape pomaces. *Industrial Crops and Products, 49*, 286–291.

Michud, A., Hummel, M., & Sixta, H. (2016b). Influence of process parameters on the structure formation of man-made cellulosic fibers from ionic liquid solution. *Journal of Applied Polymer Science, 133*(30), 1–9. https://doi.org/10.1002/app.43718

Michud, A., Tanttu, M., Asaadi, S., Ma, Y., Netti, E., Kääriainen, P., Persson, A., Berntsson, A., Hummel, M., & Sixta, H. (2016a). Ioncell-F: Ionic liquid-based cellulosic textile fibers as an alternative to viscose and Lyocell. *Textile Research Journal, 86*(5), 543–552. https://doi.org/10.1177/0040517515591774

Mikkilä, J., Trogen, M., Koivu, K. A. Y., Kontro, J., Kuuskeri, J., Maltari, R., Dekere, Z., Kemell, M., Mäkelä, M. R., Nousiainen, P. A., Hummel, M., Sipilä, J., & Hildén, K. (2020). Fungal treatment modifies kraft lignin for lignin- and cellulose-based carbon fiber precursors. *ACS Omega, 5*, 6130–6140. 10.1021/acsomega.0c00142.

Mollaee, M., Mobli, A., Mutti, N. K., Manalil, S., & Chauhan, B. S. (2019). Challenges and opportunities in cotton production. In K. Jabran, & B. S. Chauhan (Eds.), *Cotton production* (pp. 371–390). London, UK: John Wiley & Sons Ltd.. https://doi.org/10.1002/9781119385523.ch18

Moriam, K., Rissanen, M., Sawada, D., Altgen, M., Johansson, L.-S., Evtyugin, D. V., Guizani, C., Michael Hummel, M., & Sixta, H. (2021). Hydrophobization of the man-made cellulosic fibers by incorporating plant-derived hydrophobic compounds. *ACS Sustainable Chemistry & Engineering, 9*, 4915–4925. https://doi.org/10.1021/acssuschemeng.1c00695

Parviainen, A., Wahlström, R., Liimatainen, U., Liitiä, T., Rovio, S., Helminen, J. K. J., Hyväkkö, U., King, A. W. T., Suurnäkki, A., & Kilpeläinen, I. (2015). Sustainability of cellulose dissolution and regeneration in 1,5-diazabicyclo[4.3.0]non-5-enium acetate: a batch simulation of the IONCELL-F process. *RSC Advances, 5*(85), 69728–69737. https://doi.org/10.1039/c5ra12386k

Perumal, Y., & Dharmarajan, S. (2005). Betulinic acid and its derivatives: A review on their biological properties. *Current Medicinal Chemistry, 12*(6), 657–666. https://doi.org/10.2174/0929867053202214, 2005.

Portugal, I., Dias, V. M., Duarte, R. F., & Evtuguin, D. V. (2010). Hydration of cellulose/silica hybrids assessed by sorption isotherms. *The Journal of Physical Chemistry. B, 114*, 4047–4055. https://doi.org/10.1021/jp911270y

Protz, R., Lehmann, A., Ganster, J., & Fink, H.-P. (2021). Solubility and spinnability of cellulose-lignin blends in aqueous NMMO. *Carbohydrate Polymers, 251*, 117027. https://doi.org/10.1016/j.carbpol.2020.117027

Rebuzzi, F., & Evtuguin, D. V. (2005). Effect of glucuronoxylan on the hornification of *Eucalyptus globulus* bleached pulps. *Macromolecular Symposia, 232*, 121–128. https://doi.org/10.1002/masy.200551414

Sanders, D., Grunden, A., & Dunn, R. R. (2021). A review of clothing microbiology: The history of clothing and the role of microbes in textiles. *Biology Letters, 17*, Article 20200700. https://doi.org/10.1098/rsbl.2020.0700

Sawada, D., Yoshiharu Nishiyama, Y., Röder, T., Porcar, L., Zahra, H., Trogen, M., Sixta, H., & Hummel, M. (2021). Process-dependent nanostructures of regenerated cellulose fibres revealed by small angle neutron scattering. *Polymer, 218*, Article 123510. https://doi.org/10.1016/j.polymer.2021.123510

Shen, L., Worrell, E., & Patel, M. K. (2010). Environmental impact assessment of man-made cellulose fibres. *Resources, Conservation and Recycling, 55*(2), 260–274. https://doi.org/10.1016/j.resconrec.2010.10.001

Sixta, H., Michud, A., Hauru, L., Asaadi, S., Ma, Y., King, A. W. T., Kilpeläinen, I., & Hummel, M. (2015). Ioncell-F: A high-strength regenerated cellulose fibre. *Nordic Pulp and Paper Research Journal, 30*(1), 43–57. https://doi.org/10.3183/npprj-2015-30-01-p043-057

Statista. Global cotton production volume from 1990/1991 to 2023/2024 (2024). https://www.statista.com/statistics/259392/cotton-production-worldwide-since-1990/.

Stepan, A. M., Michud, A., Hellstén, S., Hummel, M., & Sixta, H. (2016). IONCELL-P&F: Pulp fractionation and fiber spinning with ionic liquids. *Industrial & Engineering Chemistry Research, 55*(29), 8225–8233. https://doi.org/10.1021/acs.iecr.6b00071

Sular, V., & Devrim, G. (2019). Biodegradation behaviour of different textile fibres: Visual, morphological, structural properties and soil analyses. *Fibres and Textiles in Eastern Europe, 27*(1), 100–111. https://doi.org/10.5604/01.3001.0012.7751

Szostak-Kotowa, J. (2004). Biodeterioration of textiles. *International Biodeterioration and Biodegradation, 53*, 165–170. https://doi.org/10.1016/S0964-8305(03)00090-8

Zhang, J., Wu, J., Yu, J., Zhang, X., He, J., & Zhang, J. (2017). Application of ionic liquids for dissolving cellulose and fabricating cellulose-based materials: State of the art and future trends. *Materials Chemistry Frontiers, 1*(7), 1273–1290. https://doi.org/10.1039/c6qm00348f